HOKKAIDO UNIVERSITY

Title	Size distributions of dicarboxylic acids and inorganic ions in atmospheric aerosols collected during polar sunrise in the Canadian high Arctic
Author(s)	Kawamura, Kimitaka; Narukawa, Masahiro; Li, Shao-Meng et al.
Citation	Journal of Geophysical Research, 112(d10), D10307 https://doi.org/10.1029/2006JD008244
Issue Date	2007-05-23
Doc URL	https://hdl.handle.net/2115/25173
Rights	An edited version of this paper was published by AGU. Copyright 2007, American Geophysical Union, JOURNAL OF GEOPHYSICAL RESEARCH, VOL. 112, D10307
Type	journal article
File Information	JGRA112-D10.pdf

Hokkaido University Collection of Scholarly and Academic Papers : HUSCAP

Size Distributions of Dicarboxylic Acids and Inorganic Ions in Atmospheric Aerosols Collected During Polar Sunrise in the Canadian High Arctic

Kimitaka Kawamura[1,*], Masahiro Narukawa[1, 2, 4], Shao-Meng Li[3] and Leonard A. Barrie[3, 5]

[1] Institute of Low Temperature Science, Hokkaido University, Sapporo, 060-0819, Japan

[2] Graduate School of Environmental Earth Science, Hokkaido University, Sapporo, 060-0810, Japan

[3] Air Quality Research Division, Atmospheric Science and Technology Directorate, Science and Technology Branch, Environment Canada, Toronto, Ontario M3H 5T4, Canada

[4] Now at Solar-Terrestrial Environment Laboratory, Nagoya University, Aichi, Japan

[5] Now Director, Atmospheric Research and Environment Programme, World Meteorological Organization, Geneva, Switzerland

* Corresponding author (kawamura@lowtem.hokudai.ac.jp)

running title: size distribution of diacids

(Manuscript Number: 2006JD008244R, Submitted to J. Geophys. Res. 12 October 2006, revised 13 January 2007, accepted 23 January 2007)

Abstract

Size-segregated atmospheric aerosols (11 stages separating particles from < 0.04 μm to > 14.2 μm) collected in the Arctic during the polar sunrise at Alert were analyzed for aerosol mass, dicarboxylic acids and major inorganic ions. Oxalic, malonic, succinic and glutaric acids were detected in all size ranges, with oxalic acid being dominant. Their concentrations maximized in the accumulation mode either at 0.24-0.40 or 0.40-0.8 μm aerodynamic diameters, suggesting that diacids were mainly formed by gas-to-particle conversion via photochemical oxidation of NMHCs and oxygenated organics originated from continental pollution sources. The relative abundances of oxalic acid were higher in the 0.24-0.4 μm size particles (73-78%) than in supermicrometer particles (40-60%), indicating that oxalic acid is produced by gas phase oxidation of precursors followed by accumulation on pre-existing particles. Mass size distributions of NH_4^+ and SO_4^{2-} peaked in the accumulation mode similar to those of small diacids. The sea-salt enrichment factor of K^+ (biomass burning tracer) relative to Na^+ maximized in 0.1-0.8 μm sizes whereas those of Mg^{2+} and Ca^{2+} (dust tracers) in 0.4-7.8 μm particles. Maximized chlorine-loss and bromine-enrichment were found at 0.4-0.8 μm and 0.24-0.4 μm sizes, respectively. Concentrations of Br^-, which typically showed a submicrometer maximum, increased significantly during an O_3 depletion event having a shift of size distribution to a supermicrometer mode. During this event, oxalic acid concentration relative to succinic acid increased in submicrometer mode (0.24-0.4 μm), adding to a growing body of evidence supporting the hypothesis that halogen chemistry is important in the production and loss of oxalic acid in the arctic atmosphere.

1. Introduction

During the polar sunrise season, the arctic troposphere can be considered as a unique chemical reactor influenced by emissions both from human activity in the mid/high latitudes and from natural sources in the Arctic Ocean. Industrialized countries in Europe, North America and Asia emit gaseous and particulate pollutants, which are transported to the Arctic during winter to spring [e.g., Barrie et al., 1989; Sirois and Barrie, 1999]. In winter, the arctic air is isolated from the Arctic Ocean water because the ocean is covered with sea ice. Furthermore, sunlight-induced chemical reactions in the atmosphere are depressed and the removal of aerosols by dry and wet deposition is much slower than at lower latitudes. Thus, photochemically reactive gases and aerosols that are transported long distances from mid-latitudes can accumulate in the arctic atmosphere before polar sunrise. Observations of unusually low ozone mixing ratios in the arctic marine boundary layer at the time of polar sunrise were first reported in the mid 1980s [Oltmans and Komhyr, 1986; Bottenheim et al., 1986]. Linkage of the ozone depletion events with concurrent peaks in filterable (i.e., particulate Br^- and HBr) bromine led to the hypothesis that ozone is consumed via a chain reaction involving Br and BrO [Barrie et al., 1988]. However, important details of the overall process remain still poorly understood despite that evidence of bromine chemistry is growing [e.g., McConnel et al., 1992; Hausmann and Platt, 1994; Impey et al., 1999; Mochida et al., 2000; Spicer et al., 2002].

Organic compounds also participate in surface ozone depletion events in the Arctic together with halogen compounds. Jobson et al. [1994] shoswed a decrease in the concentrations of non-methane hydrocarbons (NMHCs) and their compositional changes during low-ozone periods in the arctic spring. A strong positive correlation was also found between the concentrations of particulate Br and low molecular weight (LMW) dicarboxylic acids in the arctic winter to spring [Kawamura et al., 1995]. During polar sunrise, concentrations of small diacids have been reported to increase drastically by a factor of 5-20 [Kawamura et al., 1995]. Such an increase was attributed to photochemical production of diacids via the oxidation of anthropogenic organic precursors that are transported from mid

and high latitudes. If volatile organic compounds are the major precursors of the diacids, gas-to-particle conversion should play an important role, leading to an increase of particulate diacids in the submicrometer sizes. On the other hand, heterogeneous reactions may result in the production of diacids on supermicrometer particles as well. However, there is no high-resolution size distribution data for diacids in the arctic atmosphere at polar sunrise, although fine (< 1 μm) and coarse (> 1 μm) aerosols were studied in the Arctic [Narukawa et al., 2003a; Kawamura et al., 2005] where small diacids are mostly present as fine particles less than 1 μm.

In order to improve our understanding of the secondary production of LMW dicarboxylic acids during arctic polar sunrise, we have collected three sets of 11 stage size-segregated aerosol samples during the spring season of 1997. Here, we report results for LMW dicarboxylic acids and inorganic ions, and discuss possible formation mechanisms of diacids in relation to halogen chemistry. During the sampling period, significant ozone depletion events occurred in the lower arctic troposphere. The size and molecular distributions of LMW dicarboxylic acids in the arctic aerosols will be discussed in detail to better understand photochemical production and degradation during ozone depletion events. This provides additional insight into the formation mechanism of dicarboxylic acids. The size distributions of inorganic ions are also presented to better interpret the sources of the aerosol particles.

2. Samples and Method

Aerosol samples were collected in late March to mid April 1997 at Alert (82.5°N, 62.3°W) as part of the Polar Sunrise Experiment 1997 (PSE97). The sampling site is located near the Special Study Trailer (175 m a.s.l.), which is approximately 6 km south-southeast of the main military base at Alert, Nunavut, Canada. Aerosol particles were segregated at aerodynamic cut sizes of 0.04, 0.07, 0.13, 0.24, 0.4, 0.8, 1.4, 2.4, 4.9, 7.8 and 14.2 μm and were collected on the pre-combusted (450℃, 3 hrs) aluminum foils using Micro Orifice Uniform Deposit Impactor (MOUDI, MSP Corporation) at a flow rate of 30 liter/min. Three

sets of aerosol samples were collected on 29 March to 3 April (DOY 87-93), 3-9 April (DOY 93-99), and 9-14 April (DOY 99-104). The aerosol samples were stored in a clean glass vial with a Teflon-lined screw cap and shipped to the laboratory in Sapporo under freezing condition. Each aluminum foil sample was weighed before and after the sample collection using an electric micro-balance (detection limit: 10 μg) to obtain aerosol masses for each stage. Samples were stored in darkness at –20℃ until analysis.

The samples were analyzed using the method described in Narukawa et al. [2003a] and Kawamura et al. [2005]. Briefly, aliquots of aerosol samples were extracted with Milli Q water under ultra sonication. The extracts were concentrated to almost dryness by a rotary evaporator under vacuum, to which 14 % borontrifluoride in n-butanol (ca. 0.2 ml, Alltech Associates, Inc.) was added. The extracts and reagent were mixed under ultrasonication and then heated at 100℃ for 1 hour to derive carboxylic acids to butyl esters. The esters were extracted with n-hexane (10 ml) after adding Milli Q water (10ml) and acetonitrile (0.2 ml). The n-hexane layer was washed with pure water (10 ml x 4). The esters were concentrated using a rotary evaporator under vacuum, dried under nitrogen flow, and then dissolved in n-hexane (50 μl). The butyl esters were determined using a capillary GC (Hewlett-Packard, HP6890) equipped with a split/splitless injector, fused-silica capillary column (HP-5, 25 m x 0.2 mm i.d. x 0.52 μm film thickness) and an FID detector. The identification of the compounds was performed with a GC/MS (ThermoQuest, Voyager) equipped with an on-column injector and fused silica capillary column (DB-5MS, 60m x 0.32mm i.d. x 0.25 μm film thickness) using authentic dicarboxylic acid dibutyl ester standards.

Recoveries of authentic dicarboxylic acid standards spiked onto a pre-combusted quartz fiber filter were 70 % for oxalic (C_2) acid, and better than 90 % for succinic (C_4) and adipic acids. Procedural blanks showed small peaks of oxalic, succinic, and adipic acids in the GC chromatograms. However, their blank levels were almost constant and generally <10 % of those for the aerosol samples. The concentrations of the diacids reported here are corrected for the procedural blanks. The relative standard deviation of the diacid measurements based on duplicate analysis of the aerosol samples was generally 10 %.

For ion analysis, the aerosol samples were ultrasonically extracted with Milli Q water in plastic containers. The extracts were filtered with a preparation disk filter (GL Sciences, Chromatodisk 13AI). Major anions (Cl^-, Br^-, NO_3^-, and SO_4^{2-}) and cations (Na^+, K^+, Mg^{2+}, and Ca^{2+}) were determined by ion chromatography (Dionex, DX-500). For anion analysis, Dionex-AS12A column and auto-suppressor ASRS-1 were used with eluent of 4.05 mM Na_2CO_3/0.45 mM $NaHCO_3$. For cation analysis, Dionex-CS12A column and auto-suppressor CSRS-ULTRA were used with an eluent of 20.5 mM methanesulfonic acid. The injection loop volume was 500 μl for both columns. Procedural blanks showed small peaks of Cl^-, SO_4^{2-} and Ca^{2+} in the ion chromatograms. They were less than 5% of those for the aerosol samples except for Na^+, NH_4^+ and K^+ in the first set samples that were extracted with glass vials. The data for these cations in the first set samples were not used in this study. The concentrations of the ions reported here are corrected for the procedural blanks.

3. Results and Discussion

3.1. Size distribution of aerosol and soluble inorganic ion mass

Table 1 gives concentrations of aerosol mass and major ions for 11 stages of MOUDI samples. Figure 1 presents size distributions of aerosol mass concentrations (dC/dlogD, ng m^{-3}) for the size ranges from 0.04 μm to >14.2 μm in diameter for three sets of samples. The first set of aerosol samples (DOY 87-93, March 29-April 3) shows a unimodal distribution with a sharp peak at the submicrometer size at 0.4-0.8 μm in diameter. The aerosol masses for the particles less than 0.13 μm and larger than 14.2 μm are negligible, although the particles less than 0.04 μm were not collected. The second set of samples (DOY93-98, April 3-9) shows a size distribution similar to the first set, but the supermicrometer size particles (1.4-2.4 μm, 2.4-4.9 μm and larger than 14.2 μm) became more abundant, showing a bimodal distribution. The third set (DOY99-104, April 10-15) presents a broader size distribution with lower aerosol mass concentration at submicrometer size (0.4-0.8 μm) and higher concentration at supermicrometer size (2.4-4.9 μm). This sample set shows tri-modal size distribution with a maximum in the submicrometer fraction (0.4-0.8 μm) (see Figure 1).

Figure 2 shows size distributions of anions in the arctic aerosol samples. Cl^- and NO_3^- show a peak on the supermicrometer mode around 1.4-2.4 or 2.4-4.9 μm throughout the campaign. In contrast, SO_4^{2-} peaked on submicrometer mode (0.4-0.8 μm) in three sample sets. Br^- showed a submicrometer maximum in the first and third sets of samples; however, this halogen species showed a large peak at supermicrometer size during April 6-9 (DOY93-99, the second set of samples), when significant ozone depletion down to below the detection limit (1 ppbv) was observed [Narukawa et al., 2003a]. An increase in particulate Br^- concentrations may be involved with the production of Br_2 by the reaction of ozone with sea salt [Mochida et al., 2000]. Size distributions of anions (Na^+, K^+, Mg^{2+}, Ca^{2+}, NH_4^+) are shown in Figure 3. The alkaline metal ions all show a peak at supermicrometer sizes (1.4-4.9 μm), being different from SO_4^{2-} (Figure 2d). Interestingly, Mg^{2+} and Ca^{2+} that are abundant in soil dusts showed a peak shift to larger particle size from early to mid April (Figure 3c,d). NH_4^+ showed a major peak on accumulation mode (0.24-0.8 μm) and also a minor peak on supermicrometer mode. SO_4^{2-} and NH_4^+ would form ammonium sulphate salts and be present as submicrometer particles. Na^+ and Cl^-, which are both of sea salt origin, showed a peak on supermicrometer mode (1.4-4.9 μm). A small peak was found in submirometer size (0.1-0.2 μm) on DOY 99-104 (see Figure 3a). This may be a possible sampling artifact because some of the sea-salt particles may bounce off the aluminum foils in the upper impactor stages and be captured at the lower stages.

To better understand the sources of chemical components in size-segregated particles as well as depletion/enrichment of halogen species at polar sunrise, selected aerosol species in the 11 stages of DOY 93-99 and DOY 99-104 samples were compared with seawater composition. Table 2 presents sea-salt enrichment factors for aerosol species relative to Na^+ (EFss) defined as the mass ratios of species/Na^+ in aerosols divided by those in sea-salt aerosols, whose chemical composition is assumed to be equal to that of seawater [Mouri et al., 1993; Mulvaney et al., 1993]. The EFss of K^+ that is abundant in biomass burning plumes [e.g., Andreae et al., 1988] show values >1 with higher ratios (5-10) in submicron sizes (0.1-0.8 μm), suggesting that biomass burning is an important contributor to the spring arctic

aerosols. Aerosol species apportionment analysis using fifteen years of Alert observations [Sirois and Barrie, 1999] showed that, on average, in the winter aerosol K^+ mass is split between three components: unmodified Sea Salt (~50%), Mixed Photo-S/Sea Salt (~25%) and ANTHRO-S (~25%). The latter is likely an internal mixture containing wood-burning K^+ and anthropogenic sulfate formed from gas to particle conversion of SO_2 during transport to the Arctic.

Mg^{2+} and Ca^{2+} generally show higher EFss in supermicrometer sizes (e.g., 2.0 and 7.1 in DOY 99-104 sample, respectively), although relatively high values were also found in submicrometer sizes (see Table 2). These results are consistent with previous findings that long-range atmospheric transport of soil dust particles is also an important component of arctic aerosols in spring [Barrie and Barrie, 1990; Sirois and Barrie, 1999].

In contrast, EFss of Cl^- showed low values less than unity (e.g., 0.03-0.8) in submicrometer (0.4-0.8 μm) to supermicrometer (2.4-4.9 μm) sizes (Table 2). The depletion of Cl^- has been explained by the reaction with sea salt particles and sulfate based on the bulk aerosol and individual particle studies [e.g., McInnes et al., 1994; Suzuki et al., 1995]. Evidence for depletion has also been found from a component analysis of 15 years of bulk aerosol samples from Alert [Sirois and Barrie, 1999]. The present size-segregated aerosol study demonstrates that chlorine loss occurs more seriously in the particle sizes of 0.4-2.4 μm, although EFss of SO_4^{2-} maximize at smaller sizes (0.24-0.4 μm) (see Table 2). This suggests that chlorine loss is also contributed by nitrate [Pio and Lopes, 1998], whose concentrations are higher than sulfate in 1.4-2.4 and 2.4-4.9 μm sizes (see Table 1 and Figure 2). Interestingly, higher EFss values of Cl^- were also observed in some sub- and super-micrometer sizes, suggesting that HCl gas is deposited on both mode particles. On the other hand, Br^- showed very high EFss values up to 70 in submicrometer sizes (e.g., 0.24-0.4 μm) especially when serious ozone depletion was observed (DOY93-99). It is of interest to note that the Br enrichment occurs on the particle sizes smaller than those where Cl-loss occurs. Although Cl-loss and Br-enrichment have been reported in the fine and coarse aerosols in the Arctic [Barrie et al., 1994], this study report, for the first time, their detailed

EFss over the 11-stages of particle sizes and their dependence on particle sizes.

3.2 Size distribution of dicarboxylic acids

Homologous α,ω-dicarboxylic acids (C_2-C_9) were detected in the size-segregated samples. Concentrations of individual dicarboxylic acids in each stage are given in Table 1. Throughout the sampling periods, oxalic acid was found as a dominant species followed by C_3 or C_4 diacid in most of the segregated aerosol fractions. These results are consistent with previous observations of the bulk [Kawamura et al., 1996] and fine/coarse aerosols at this location [Narukawa et al., 2003a; Kawamura et al., 2005]. However, longer-chain diacids such as C_7-C_9 in the MOUDI samples were often below the detection limit (ca. 0.01 ng m^{-3}), most likely due to the limited volume of air sampled for multiple stages. The total concentrations of the diacids in the MOUDI samples were found to be 2-3 times lower than those obtained for daily samples collected simultaneously at the same site using a high volume sampler [Narukawa et al., 2003a], although the sampling intervals are not equivalent. Lower concentrations of diacids have been reported in the aerosol samples collected using impactor samplers [Kerminen et al., 2003]. This may be caused by the potential discriminative loss of larger size particles and evaporative loss for fine particles under the condition of decreased pressure inside the impactor sampling system.

Figure 4 shows the mass size distribution of individual C_2-C_5 dicarboxylic acids collected during three sampling periods. The present study based on MOUDI sampling clearly shows that the aerosol diacid concentrations maximize in accumulation mode size range of 0.4-0.8 μm and confirms the previous conclusion that in the Arctic, aerosols are mostly present in fine particles [Narukawa et al., 2003a; Kawamura et al., 2005]. The submicrometer maxima of small diacids suggest that they are secondary products in the atmosphere formed from photochemical oxidation of gaseous precursors during long-range transport and/or in the Arctic. Interestingly, EFss calculated for C_2-C_4 diacids showed values much greater than 1 with maxima in the submicrometer size range of 0.24-0.4 μm (see Table 2). Thus, the present study demonstrates that they are clearly not of sea salt origin, which is consistent with our

conclusion that they are largely produced in the atmosphere. The total diacid concentrations in the MOUDI samples were highest during Days 87-93 and decreased during DOY 93-99 and 99-104 (Table 1).

Kerminen et al. [1999] studied dicarboxylic acids in the aerosols collected in the lower Arctic at Sevettijärivi, Northern Finland (69°N, 28°E) during the summer season and found a concentration peak in the supermicrometer size range. Since the samples were collected in the season affected by continental and marine air masses, dicarboxylic acids are expected to exist in supermicrometer mode of aerosols transported from lower and mid latitudes. The shift of small diacids from submicrometer to supermicrometer mode has been observed in coastal marine aerosols collected from the western North Pacific during the spring season when a strong outflow of Asian dusts occurred [Mochida et al., 2003]. In this study at Alert, dicarboxylic acids did not show a peak in the supermicrometer mode but peaked in the submicrometer mode. These results suggest that LWM diacids in the arctic aerosols were formed by gas-to-particle conversion reactions in the marine boundary layer over the Arctic Ocean. However, they were not influenced markedly by sea salt particles, which may cause the shift of small diacids to the supermicrometer mode. This is because the Arctic Ocean is still covered with sea ice in spring and the sea salt emission to the atmosphere is low during the sampling periods.

Figure 5 presents the percentage relative abundance of individual C_2-C_5 diacids in aerosol mass as a function of particle size for the three sample sets. Ultra fine fractions (0.04-0.07 μm and 0.07-0.13 μm) in the DOY 87-93 sample showed the highest values (3.4-3.5%); the other fractions generally showed values less than 0.6%. The sample set from DOY 93-99, collected when serious ozone depletion down to below detection limit (< 1 ppbv O_3) occurred [see Figure 7 in Narukawa et al., 2003a], showed the highest values (ca. 0.7%) at 0.24-0.4 μm size and lower values in smaller and larger size ranges. This suggests that LMW diacids produced via photochemical processes are more accumulated on the submicrometer mode rather than supermicrometer mode. Although the sample set of DOY 99-104 showed a high percentage in the 0.07-0.13 μm size range, it may be an artifact

because aerosol mass concentration may have been seriously underestimated by uncertain measurement by chance because mass concentration value of this size range is extremely low (see Table 1). In the same sample set, the large sizes (>14.2 μm) showed a high value (ca. 0.5%), suggesting that small diacids may be in part shifted to the larger particle size during the prolonged residence in the arctic atmosphere. Redistribution of small diacids from fine to coarse mode has been discussed in the remote marine aerosols [Mochida et al., 2003].

3.3. Molecular compositions and formation pathways of particulate dicarboxylic acids

Although LMW dicarboxylic acids detected on the accumulation mode size in the arctic aerosol samples showed a predominance of oxalic acid, their chain-length distributions are found to be variable depending on the particle size. Figure 6 shows changes in the C_2/C_4 and C_3/C_4 concentration ratios as a function of particle size. The C_2/C_4 ratios in the first sample set (DOY 87-93) increase from ultra fine particle size (0.04-0.07 μm) toward larger size (0.8-1.4 μm) with the maximum of 13 at the submicrometer size (0.24-0.4 μm) (Figure 6a). Similar trend was obtained in the other two sample sets (DOY 93-99 and 99-104); however, a big jump of the C_2/C_4 ratio (23) was observed at the submicrometer size (0.24-0.4 μm) during DOY 93-99 when a major O_3 depletion was observed. Although a previous Alert aerosol study demonstrated that concentrations of small diacids (C_2-C_5) in the fine fraction increased during an O_3 depletion/Br increase event [Narukawa et al., 2003a], this study of high resolution size distribution clearly showed that oxalic acid is preferentially produced over C_4 diacid and/or C_4 is selectively decomposed in the submicrometer size (0.24-0.4 μm) and that this process is intensified during an O_3 depletion/Br increase event.

One explanation for this is that photochemical oxidation of NMHCs and other volatile organics leads to higher relative production of oxalic acid and it accumulates in the fine particle size around 0.2-0.4 μm. The photochemical production of oxalic acid in the fine particle size may be involved with surface O_3 depletion, which is coupled with chemical mechanisms leading to Br^- formation. Although Br^- is mostly detected in supermicrometer sizes (1.4-2.4 μm and 2.4-4.9 μm, see Figure 2b and Table 1) during the O_3 depletion event,

production of Br_2 and/or BrO [McConnel et al., 1992; Hausmann and Platt, 1994; Spicer et al., 2002] may be responsible for the formation of oxalic acid at the polar sunrise season. In the previous paper [Narukawa et al., 2003a], we proposed reaction mechanism of bromine chemistry for the production of small diacids from the precursors containing aldehydes functional group (e.g., glyoxal, glyoxylic acid) as below.

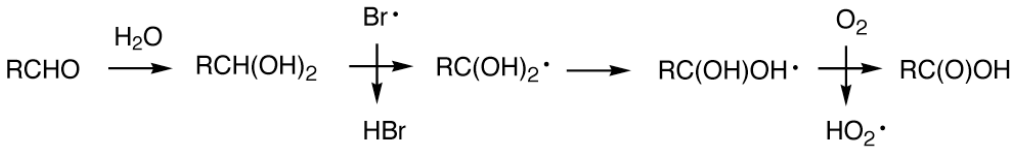

This mechanism is consistent with independent evidence that brominated diacids were detected in the arctic aerosols [Narukawa et al., 2003b] and with proposed heterogeneous reactions that aldehyde functional group is oxidized to carboxyl group on aerosol surface [Warneck, 2003].

As mentioned above, we observed that concentration of oxalic acid relative to succinic acid increased in the fine aerosols (0.24-0.4 μm) during ozone depletion period and concentration of Br^- simultaneously increased in the coarse aerosols. HBr gas that is released by the reaction described above should react with slightly alkaline particles of sea salt origin, which are present on the coarse (1.4-2.4 and 2.4-4.9 μm) mode where Na and Cl ions are enriched (see Figures 2a and 3a). This is consistent with the present observation that during ozone depletion event (DOY 93-99, Figure 2b), non-sea salt Br^- was peaked in the coarse fraction (1.4-2.4 μm and 2.4-4.9 μm, Figure 2b). Although glyoxylic acid and other intermediate compounds were not measured in this study due to the limited volume of air collected, we detected higher concentrations of oxalic and glyoxylic acids and lower concentrations of unsaturated structures (maleic and phthalic acids) in the aerosol samples simultaneously collected at the same site using high volume sampler on daily basis during an ozone depletion events (April 7-8 1997) [Kawamura et al., unpublished data]. The unsaturated compounds can serve as precursors of glyoxal and glyoxylic acid which are further oxidized to oxalic acid during ozone depletion event involved with bromine chemistry [Kawamura et

al., 1996, 2005].

In the three sets of samples, a similar trend to that for C_2/C_4 was also found for the C_3/C_4 ratio in the fine particle size of 0.24-0.4 μm (Figure 6b). A large increase in the ratio was found in the second sample set (DOY 93-99) when the O_3 depletion event occurred under a situation similar to the case of the C_2/C_4 ratio. This again suggests that LMW diacids such as C_2 and C_3 are preferentially produced over succinic acid (C_4) and/or C_4 is preferentially decomposed in the submicrometer particle size. It is of interest to note that the relative abundance of C_4 diacid in the total diacids increases from ca. 6-15% in submicrometer particles (0.24-0.4 μm) to 22-38% in supermicrometer particles (7.8-14.2 μm) in all three samples (see Figure 7), suggesting that succinic acid may be related to heterogeneous oxidation of precursor compounds such as mid-chain ketocarboxylic acids (e.g., 4-oxononanoic acid), long-chain diacids and fatty acids that are known to exist in aerosol particles [Kawamura and Gagosian, 1987, 1990; Kawamura et al., 1996b]. Heterogeneous production of C_4 diacid on the particle may also be important in the arctic atmosphere in addition to the gas-to-particle formation, although the latter is more significant in the arctic spring.

4. Summary and Conclusions

Oxalic, malonic, succinic and glutaric acids were studied in three sets of high Arctic aerosol samples size-segregated into 11 stages using a MOUDI impactor during polar sunrise season. Oxalic acid was generally the dominant species in all the segregated fractions. Small diacids (C_2-C_5) in aerosol samples showed maximum concentrations on the accumulation (submicrometer) mode between 0.24-0.8 μm aerodynamic diameters. The abundances of the diacids relative to aerosol mass generally peaked in the fine fraction (0.24-0.4 μm). Aerosols showed an enhanced production of oxalic and malonic acids relative to succinic acid in the submicrometer size. This trend was intensified when significant ozone depletion and Br increase were observed. The present study demonstrates that small diacids are produced predominantly as submicrometer aerosols by photochemically induced-reactions in the Arctic

atmosphere. Although this study emphasizes the importance of production of diacids coupled with bromine chemistry in aerosol phase, further studies are needed for a better understanding of this process.

Acknowledgements

The authors thank D. Toom-Sauntry for her support in collecting samples, and H. Narita, M. Watanabe and S. Matoba for their help in the analysis of inorganic ions. We also thank anonymous reviewer for the useful comments. This research was supported in part by the Japanese Ministry of Education, Science, Sports and Culture through Grant-in-Aid 09304054 and 10144101.

References

Andreae, M. O., E. V. Browell, M. Garstang, G. L. Gregory, R. C. Harriss, G. F. Hill, D. J. Jacob, M. C. Pereira, G. W. Sachse, A. W. Setzer, P. L. Silva Dias, R. W. Talbot, A. L. Torres, S. C. Wofsy (1988), Biomass-burning emissions and associated haze layers over Amazonia. *J. Geophys. Res*., *93*, 1509–1527.

Barrie, L. A., J. W. Bottenheim, R. C. Schnell, P. J. Crutzen, and R. A. Rasmussen (1988), Ozone destruction and photochemical reactions at polar sunrise in the lower Arctic troposphere. *Nature, 334*, 138-141.

Barrie, L. A., and M. J. Barrie (1990), Chemical components of lower tropospheric aerosols in the high Arctic: Six years of observations. *J. Atmos. Chem. 11*, 211-226.

Barrie, L. A., G. Den Hartog, J. W. Bottenheim, and S. Landsberger (1989), Anthropogenic aerosols and gases in the lower troposphere at Alert Canada in April 1986. *J. Atmos. Chem., 9*, 101-27.

Barrie, L. A., R. Staebler, D. Toom, B. Georgi, G. den Hartog, S. Landsberger, and D. Wu (1994), Arctic aerosol size-segregated chemical observations in relation to ozone depletion during Polar Sunrise Experiment 1992. *J. Geophys. Res.*, *99*, 25439-25451.

Bottenheim, J. W., A. G. Gallant, and K. A. Brice (1986), Measurements of NO_y species and O_3 at 82ºN latitude. *Geophys. Res. Lett., 13*, 113-116.

Hausmann, M., and U. Platt (1994), Spectroscopic measurement of bromine oxide and ozone in the high Arctic during Polar Sunrise Experiment 1992. *J. Geophys. Res.*, *99*, 25399-25413.

Impey, G. A., C. M. Mihele, K. G. Anlauf, L. A. Barrie, D. R. Hastie, and P. B. Shepson (1999), Measurements of photolyzable halogen compounds and bromine radicals during the polar sunrise experiment 1997. *J. Atmos. Chem., 34*, 21-37.

Jobson, B. T., H. Niki, Y. Yokouchi, J. W. Bottenheim, F. Hopper, R. Leaitch (1994), Measurements of C_2-C_6 hydrocarbons during the Polar Sunrise 1992 Experiment: evidence for Cl atom and Br atom chemistry. *J. Geophys. Res.*, *99*, 25,355-25,368.

Kawamura, K., and R. B. Gagosian (1987), Implications of ω-oxocarboxylic acids in the

remote marine atmosphere for photo-oxidation of unsaturated fatty acids. *Nature, 325*, 330-332.

Kawamura, K., and R. B. Gagosian (1990), Mid-chain ketocarboxylic acids in the remote marine atmosphere: Distribution patterns and possible formation mechanisms. *J. Atmos. Chem., 11*, 107-122.

Kawamura, K., H. Kasukabe, O. Yasui, and L. A. Barrie (1995), Production of dicarboxylic acids in the Arctic atmosphere at polar sunrise. *Geophys. Res. Lett., 22*, 1253-1256.

Kawamura, K., H. Kasukabe, and L. A. Barrie (1996), Source and reaction pathways of dicarboxylic acids, ketoacids and dicarbonyls in Arctic aerosols: one year of observations. *Atmos. Environ., 30*, 1709-1722.

Kawamura, K., Y. Imai, and L. A. Barrie (2005), Photochemical production and loss of organic acids in high Arctic aerosols during long range transport and polar sunrise ozone depletion events. *Atmos. Environ., 39*, 599-614.

Kerminen, V. –K., K. Teinilä, R. Hillamo, and T. Mäkelä (1999), Size-segregated chemistry of particulate dicarboxylic acids in the Arctic atmosphere. *Atmos. Environ., 33*, 2089-2100.

McConnel, J. C., G.S. Henderson, L. Barrie, J. Bottenheim, H. Niki, C.H. Langford, and E.M.J. Templeton (1992), Photochemical bromine production implicated in Arctic boundary-layer ozone depletion. *Nature, 355*, 150-153.

McInnes, L. M., D. S. Covert, P. K. Quinn, and M. S. Germani (1994), Measurements of chloride depletion and sulfur enrichment in individual sea-salt particles collected from the remote marine boundary layer. *J. Geophys. Res., 99*, 8257-8268.

Mochida M., J. Hirokawa, and H. Akimoto (2000), Unexpected Large Uptake of O_3 on Sea Salts and the Br_2 production, *Geophys. Res. Lett*, *27*, 2629-2632.

Mochida, M., N. Umemoto, K. Kawamura, and M. Uematsu (2003), Bimodal size distribution of C_2-C_4 dicarboxylic acids in the marine aerosols, *Geophys. Res. Lett., 30*, 1672, doi:10.1029/2003GL017451.

Mouri, H., K. Okada, and K. Shigehara (1993), Variation of Mg, S, K and Ca contents in

individual sea salt particles. *Tellus, 45(B),* 8-85.

Mulvaney, R., G. F. J. Coulson, and H. F. J. Corr (1993), The fractionation of sea-salt and acids during transport across the Antarctic ice shelf, *Tellus, 45(B),* 179-186.

Narukawa, M., K. Kawamura, K. G. Anlauf, L. A. Barrie (2003a), Fine and coarse modes of dicarboxylic acids in the Arctic aerosols collected during the Polar Sunrise Experiment 1997. *J. Geophys. Res., 108*, NO. D18, 4575, doi:10.1029/2003JD00364.

Narukawa M., K. Kawamura, H. Hatsushika, K. Yamazaki, S.-M. Li, J. W. Bottenheim and K. G. Anlauf (2003b), Measurement of halogenated dicarboxylic acids in the spring arctic aerosols, *J. Atmos. Chem*. *44*, 323-335.

Oltmans, S. J., and W. D. Komhyr (1986), Surface ozone distribution and variations from 1973-1984 measurements at the NOAA geophysical monitoring for climatic change baseline observation. *J. Geophys. Res*., *91*, 5229-5236.

Pio, C. A., and D. A. Lopes (1998), Chlorine loss from marine aerosol in a coastal atmosphere. *J. Geophys. Res*., *103D*, 25263-25272.

Sirois, A. and L.A. Barrie (1999), Arctic lower tropospheric aerosol trends and composition at Alert, Canada: 1980-1995. *J. Geophysic. Res., 104D*, 11599-11618.

Spicer, C. W., R. A. Plastridge, K. L. Foster, B. J. Finlayson-Pitts, J. W. Bottenheim, A. M. Grannas, and P. B. Shepson (2002), Molecular halogens before and during ozone depletion events in the Arctic at polar sunrise: concentrations and sources. *Atmos. Environ., 36*, 2721-2731.

Suzuki, K., K. Kawamura, H. Kasukabe, A. Yanase and L. A. Barrie (1995), Concentration changes of MSA and major ions in arctic aerosols during polar sunrise. *Proc. NIPR Symp. Polar Meteorol. Glaciol., 9*, 163-171.

Tedetti, M., K. Kawamura, B. Charriere, N. Chevalier, and R. Sempéré (2006), Determination of low molecular weight dicarboxylic acids in seawater samples, *Anal. Chem., 78*, 6012-6018.

Warneck, P. (2003), In-cloud chemistry opens pathway to the formation of oxalic acid in the marine atmosphere. *Atmos. Environ., 37*, 2423-2327.

Figure captions

Figure 1. Size distribution of aerosol mass concentrations ($dC/dlogD_p$, ng m^{-3}) in the aerosol particles collected at Alert in 1997.

Figure 2. Size distribution of concentrations ($dC/dlogD_p$, ng m^{-3}) of inorganic anions in the aerosol particles collected at Alert in 1997.

Figure 3. Size distribution of concentrations ($dC/dlogD_p$, ng m^{-3}) of inorganic cations in the aerosol particles collected at Alert in 1997.

Figure 4. Size distribution of concentrations ($dC/dlogD_p$, ng m^{-3}) of dicarboxylic acids in the aerosol particles collected at Alert in 1997.

Figure 5. Changes in the relative abundances of individual C_2-C_5 diacids in aerosol mass as a function of particle sizes.

Figure 6. Changes in the diacid composition in the MOUDI samples collected from Alert. (a) oxalic/succinic acid concentration ratios (C_2/C_4), (b) malonic/succinic acid concentrations ratios (C_3/C_4).

Figure 7. Changes in the relative abundances of individual C_2-C_5 diacids in the MOUDI samples collected from Alert.

Table 1. Concentrations (ngm-3) of aerosol mass, major ions and dicarboxylic acids in the size segregated aerosol samples collected in the Arctic, 1997.

Dates	Sampl ID	Size (μm)	Aero mass	Na	NH4	K	Mg	Ca	MSA	Cl	Br	NO3	SO4	total ions	oxalic	mal onic	succi nic	gluta ric	adipi c	pimel ic	suber ic	azelai c	Total diacids
March 28 to April 3	1	0.04 – 0.07	5	–	–	–	0.2	0.3	0.0	15.5	0.0	0.9	1.9	–	0.06	0.03	0.05	0.01	0.02	0.00	0.00	0.00	0.16
(DOY87-93)	2	0.07 – 0.13	12	–	–	–	0.8	0.4	0.0	0.0	0.0	0.0	0.0	–	0.14	0.04	0.08	0.02	0.16	0.01	0.01	0.01	0.46
	3	0.13 – 0.24	149	–	–	–	0.5	1.2	0.0	9.8	0.0	0.0	5.0	–	0.40	0.12	0.17	0.05	0.04	0.00	0.00	0.01	0.78
	4	0.24 – 0.4	465	–	–	–	1.0	1.9	0.0	11.1	3.0	2.2	69.9	–	2.10	0.40	0.16	0.04	0.02	0.00	0.00	0.00	2.72
	5	0.4 – 0.8	912	–	–	–	2.0	3.8	0.0	13.5	4.1	2.9	174.3	–	3.75	1.23	0.93	0.25	0.08	0.01	0.00	0.04	6.29
	6	0.8 – 1.4	673	–	–	–	6.1	7.9	0.0	14.8	1.8	5.7	138.3	–	2.48	0.71	0.46	0.11	0.04	0.01	0.00	0.02	3.82
	7	1.4 – 2.4	179	–	–	–	4.0	3.8	0.0	46.7	0.0	30.7	22.4	–	0.47	0.11	0.12	0.04	0.05	0.00	0.01	0.00	0.80
	8	2.4 – 4.9	157	–	–	–	2.5	3.8	0.0	62.4	0.0	20.2	11.8	–	0.18	0.05	0.05	0.01	0.02	0.00	0.00	0.00	0.32
	9	4.9 – 7.8	42	–	–	–	1.4	0.6	0.0	15.2	0.0	3.8	1.7	–	0.12	0.02	0.05	0.01	0.04	0.00	0.00	0.00	0.24
	10	7.8 – 14.2	27	–	–	–	0.8	0.6	2.0	28.0	0.0	0.9	16.5	–	0.06	0.00	0.03	0.00	0.02	0.00	0.00	0.00	0.11
	11	>14.2	0	–	–	–	0.1	0.2	0.0	16.3	0.0	3.6	0.9	–	0.13	0.03	0.06	0.02	0.02	0.00	0.00	0.00	0.26
		total (>0.04)	2619	–	–	–	19.5	24.5	2.0	233.3	8.9	71	443	–	9.89	2.74	2.16	0.54	0.51	0.03	0.02	0.08	15.97
April 3 to 9	12	0.04 – 0.07	92	6.0	4.4	0.7	0.4	0.2	0.0	15.1	0.0	0.5	0.1	27.3	0.09	0.02	0.07	0.02	0.03	0.01	0.01	0.00	0.24
(DOY93-99)	13	0.07 – 0.13	129	6.8	5.4	0.7	0.3	0.2	0.0	10.2	0.0	0.0	0.0	23.6	0.06	0.01	0.05	0.01	0.02	0.00	0.00	0.00	0.15
	14	0.13 – 0.24	198	4.0	14.0	1.0	0.5	0.2	0.0	11.9	0.6	0.0	13.9	46.1	0.42	0.13	0.07	0.02	0.02	0.00	0.00	0.00	0.66
	15	0.24 – 0.4	478	5.3	14.1	1.7	1.0	0.4	0.5	10.3	2.3	0.5	63.0	99.3	2.53	0.56	0.11	0.02	0.02	0.00	0.00	0.00	3.25
	16	0.4 – 0.8	962	10.4	48.0	4.1	2.2	1.5	1.4	11.3	3.5	1.8	190.2	274.3	2.59	1.07	0.55	0.15	0.05	0.01	0.00	0.02	4.44
	17	0.8 – 1.4	755	28.1	29.2	3.8	9.5	4.6	0.0	1.4	2.3	0.0	137.5	216.4	2.14	0.91	0.28	0.06	0.03	0.00	0.00	0.00	3.41
	18	1.4 – 2.4	468	41.3	4.0	3.1	8.7	4.6	3.6	33.5	11.1	27.2	14.9	152.1	0.19	0.09	0.13	0.04	0.02	0.00	0.00	0.00	0.47
	19	2.4 – 4.9	407	42.6	3.4	3.1	9.7	6.4	0.0	62.5	7.3	21.8	7.9	164.7	0.13	0.07	0.10	0.04	0.03	0.01	0.00	0.00	0.38
	20	4.9 – 7.8	162	15.7	11.1	1.2	3.0	2.1	0.0	32.9	0.4	7.9	2.2	76.5	0.06	0.00	0.03	0.00	0.01	0.00	0.00	0.00	0.10
	21	7.8 – 14.2	99	3.8	5.4	0.5	0.6	0.3	0.0	3.5	0.0	1.8	1.0	17.0	0.04	0.01	0.02	0.00	0.01	0.00	0.00	0.00	0.09
	22	>14.2	136	7.5	9.3	0.9	0.7	0.3	0.0	15.5	0.0	2.4	0.0	36.7	0.04	0.00	0.03	0.01	0.01	0.00	0.00	0.00	0.10
		total (>0.04)	3887	171.7	148.4	20.7	36.6	21.0	5.6	208.1	27.5	64	431	1134.0	8.30	2.87	1.44	0.37	0.26	0.03	0.01	0.02	13.30
April 9 to 14	23	0.04 – 0.07	45	6.6	2.3	0.9	0.5	0.2	0.0	15.5	0.0	0.6	0.1	26.6	0.13	0.03	0.09	0.02	0.03	0.00	0.00	0.00	0.30
(DOY99-104)	24	0.07 – 0.13	3	5.9	2.8	0.7	0.4	0.1	0.5	14.3	0.0	0.9	1.9	27.5	0.06	0.00	0.06	0.01	0.03	0.00	0.00	0.00	0.16
	25	0.13 – 0.24	132	13.1	5.8	1.8	0.7	0.5	0.0	19.9	0.0	0.0	13.7	55.4	0.23	0.09	0.06	0.01	0.02	0.00	0.00	0.00	0.41
	26	0.24 – 0.4	395	7.8	34.2	2.5	1.6	0.7	0.7	14.1	0.7	0.0	72.3	134.8	1.68	0.48	0.12	0.01	0.02	0.00	0.00	0.00	2.31
	27	0.4 – 0.8	658	26.2	33.3	4.7	3.2	3.3	4.7	2.4	0.7	0.0	126.3	204.8	1.80	0.54	0.17	0.02	0.03	0.00	0.00	0.00	2.56
	28	0.8 – 1.4	425	47.3	16.9	4.1	7.7	4.0	0.6	21.3	0.8	8.5	50.9	162.1	0.72	0.29	0.20	0.06	0.04	0.00	0.00	0.00	1.31
	29	1.4 – 2.4	436	54.7	5.4	3.0	9.3	7.8	0.0	73.8	0.0	38.6	11.5	204.0	0.23	0.11	0.15	0.06	0.03	0.00	0.01	0.00	0.59
	30	2.4 – 4.9	529	67.1	18.4	3.5	15.9	18.1	0.0	90.9	0.0	32.8	13.6	260.3	0.20	0.07	0.09	0.02	0.03	0.00	0.00	0.00	0.41
	31	4.9 – 7.8	242	31.4	3.3	1.3	4.9	8.1	0.0	57.0	0.0	7.2	3.7	117.0	0.07	0.00	0.04	0.00	0.02	0.00	0.00	0.00	0.13
	32	7.8 – 14.2	78	15.7	12.0	1.1	1.1	2.2	0.0	31.0	0.0	2.1	0.0	65.2	0.06	0.00	0.05	0.00	0.01	0.00	0.00	0.00	0.12
	33	>14.2	45	19.9	1.3	1.1	1.0	1.4	0.0	21.6	0.0	2.9	0.0	49.1	0.07	0.04	0.05	0.00	0.02	0.00	0.00	0.00	0.19
		total (>0.04)	2987	295.6	135.6	24.8	46.3	46.3	6.5	361.9	2.2	94	294	1306.7	5.26	1.67	1.08	0.22	0.27	0.00	0.01	0.00	8.49

Table 2. Sea-salt enrichment factors of selected inorganic ions and dicarboxylic acids relative to Na in the size segregated aerosols from the High Arctic (1991).											
					Enrichment factors relative to seawater Na*						
Aerosol Samples	Size (μm)	Na	K	Mg	Ca	Cl	Br	SO4	C2	C3	C4
April 3-9 (DOY 93-99)											
	0.04 - 0.07	1	3.0	0.5	1.1	1.4	0.0	0.04	12900	13000	161000
	0.07 - 0.13	1	2.7	0.3	1.0	0.8	0.0	0.0	7700	7600	97000
	0.13 - 0.24	1	6.8	1.0	1.0	1.6	23.8	13.7	87600	144000	260000
	0.24 - 0.4	1	8.9	1.6	2.1	1.1	69.9	47.0	398000	461000	291000
	0.4 - 0.8	1	10.9	1.7	3.7	0.6	53.9	72.5	208000	452000	748000
	0.8 - 1.4	1	3.8	2.8	4.3	0.03	13.0	19.5	63000	141000	141000
	1.4 - 2.4	1	2.1	1.7	2.9	0.45	43.7	1.4	3900	9600	43000
	2.4 - 4.9	1	2.0	1.9	4.0	0.8	27.8	0.7	2500	6800	35000
	4.9 - 7.8	1	2.2	1.6	3.6	1.2	4.7	0.6	3300	-	24000
	7.8 - 14.2	1	3.4	1.4	2.4	0.5	0.0	1.1	9500	12000	71000
	>14.2	1	3.3	0.8	1.2	1.1	0.0	0.0	4900	-	64000
	total (>0.04)	1	3.3	1.8	3.2	0.7	26.0	10.0	40000	73000	119000
April 9-14 (DOY 99-104)											
	0.04 - 0.07	1	3.9	0.6	0.8	1.3	0.0	0.1	16000	18000	200000
	0.07 - 0.13	1	3.2	0.6	0.6	1.4	0.0	1.3	9200	-	138000
	0.13 - 0.24	1	3.8	0.4	1.0	0.8	0.0	4.2	14000	29000	66000
	0.24 - 0.4	1	9.0	1.8	2.4	1.0	15.0	37.1	182000	271000	220000
	0.4 - 0.8	1	5.0	1.0	3.3	0.05	4.4	19.2	57000	91000	90000
	0.8 - 1.4	1	2.4	1.4	2.2	0.25	2.7	4.3	12000	27000	60000
	1.4 - 2.4	1	1.5	1.4	3.7	0.7	0.0	0.8	3500	9100	38000
	2.4 - 4.9	1	1.5	2.0	7.1	0.8	0.0	0.8	2400	4800	19000
	4.9 - 7.8	1	1.2	1.3	6.8	1.0	0.0	0.5	1900	-	19000
	7.8 - 14.2	1	1.9	0.6	3.7	1.1	0.0	0.0	3200	-	41000
	>14.2	1	1.5	0.4	1.8	0.6	0.0	0.0	2900	9800	36000
	total (>0.04)	1	2.3	1.3	4.1	0.7	1.2	4.0	14000	24000	51000
*: Seawater concentrations of C2-C4 diacids were taken from the data reported in the Mediterranean Sea (Tedetti et al., 2006).											
For the definition of enrichment factors, see section 3.1 in the text.											

Figure 1 (Kawamura et al.)

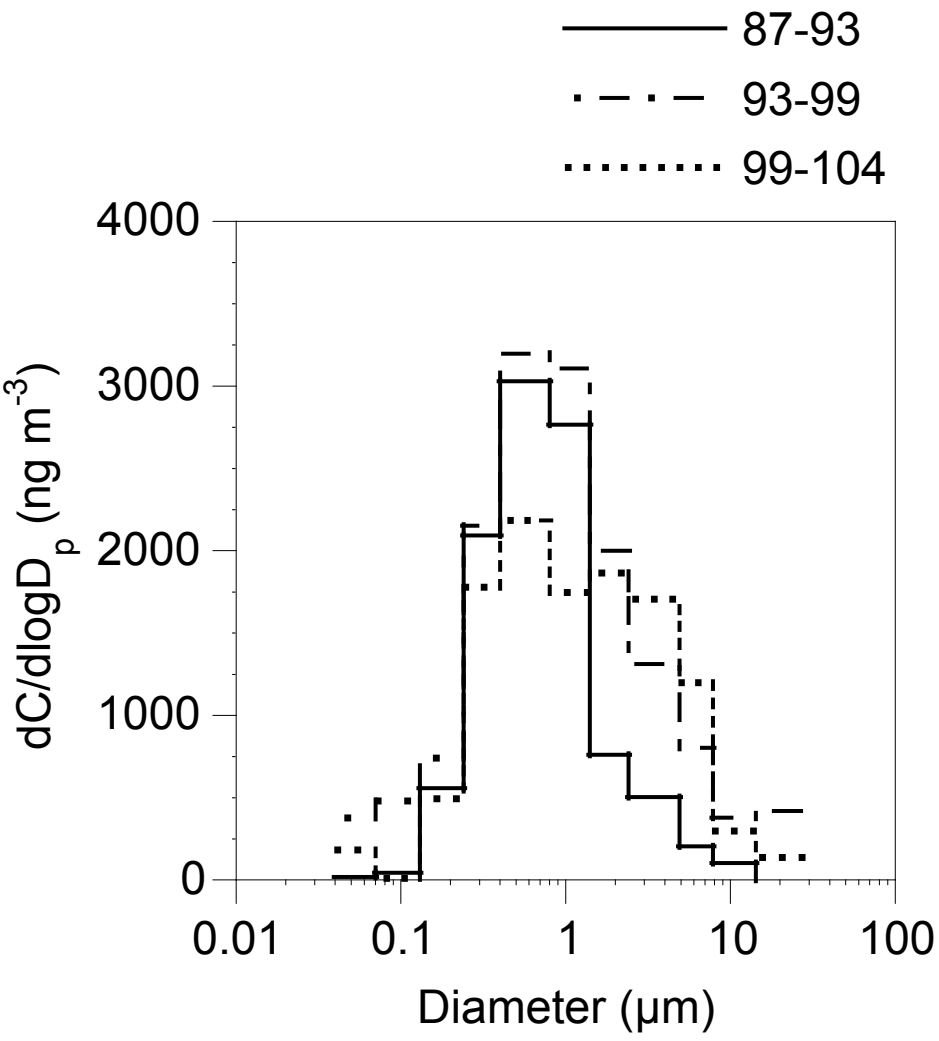

Figure 2 (Kawamura et al.)

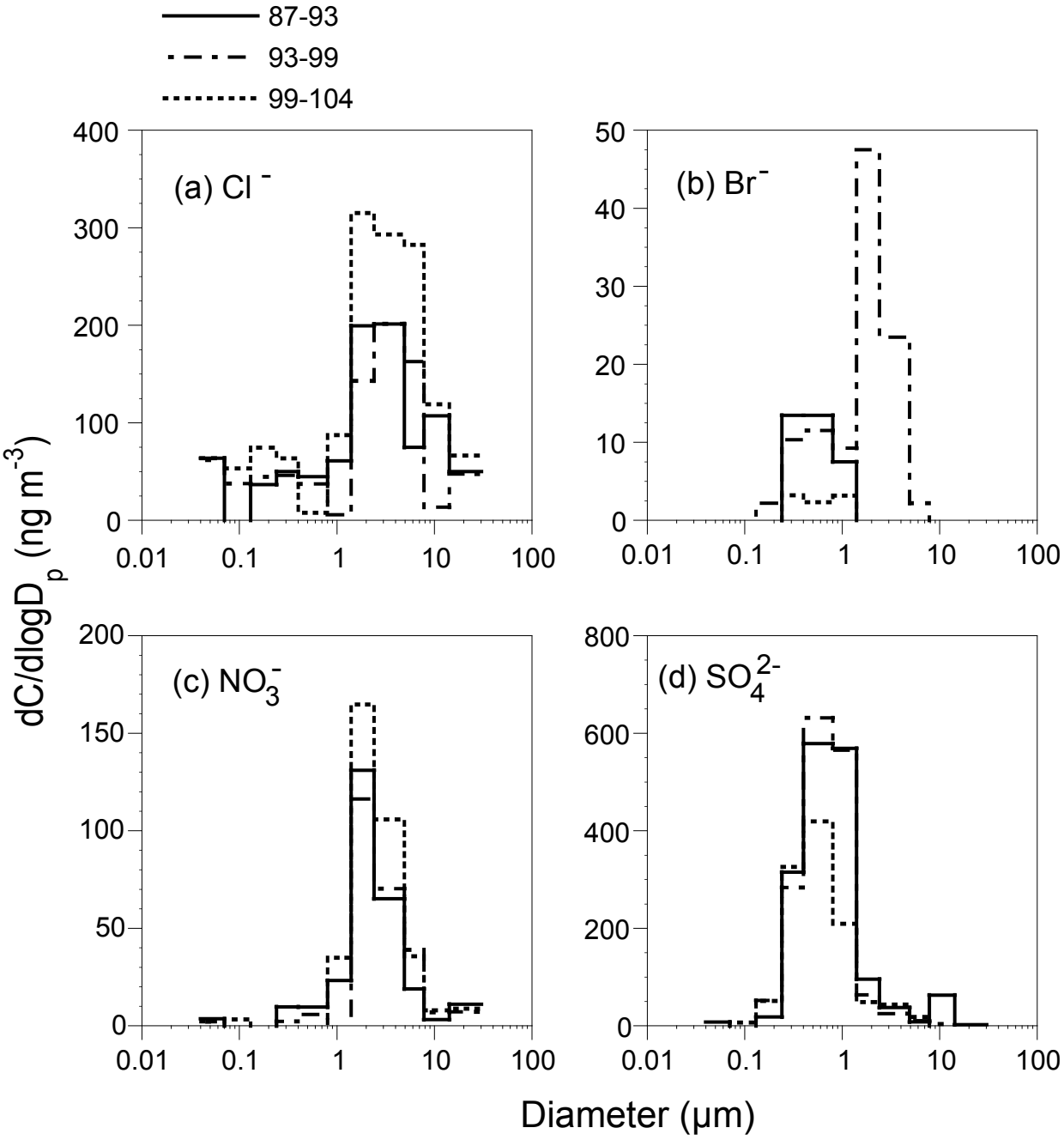

Figure 3 (Kawamura et al.)

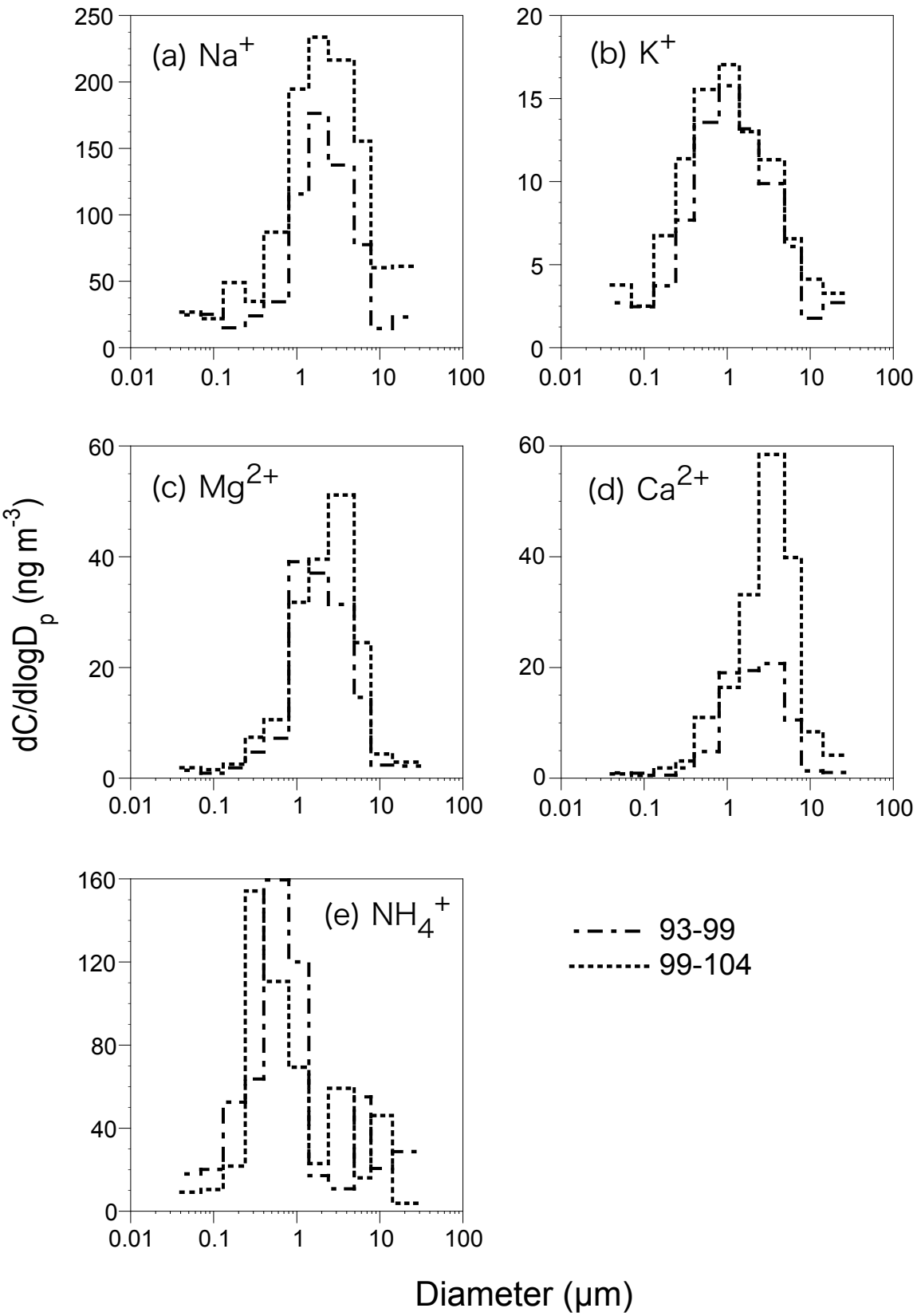

Figure 4 (Kawamura et al.)

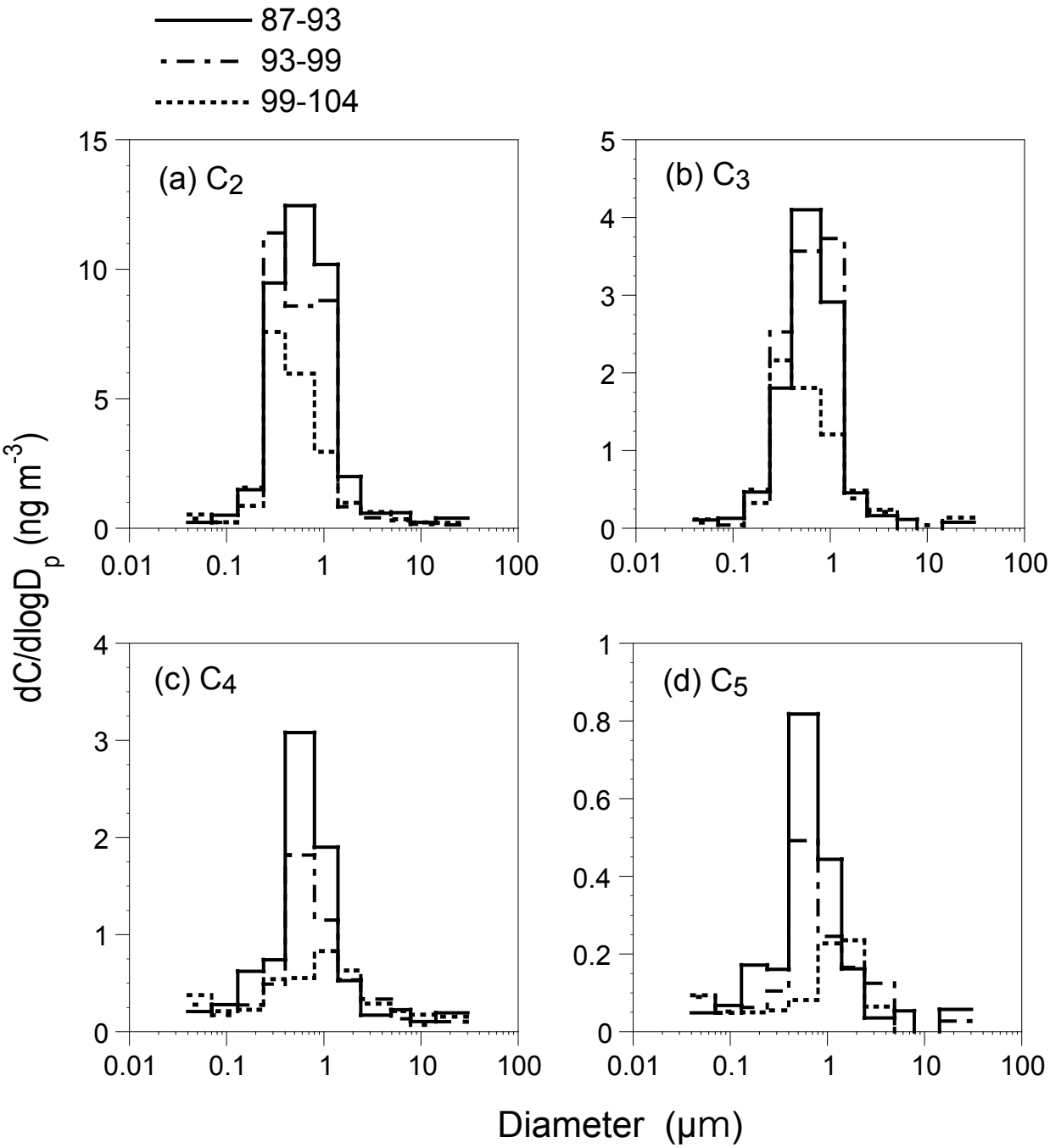

Fig. 5 (Kawamura et al.)

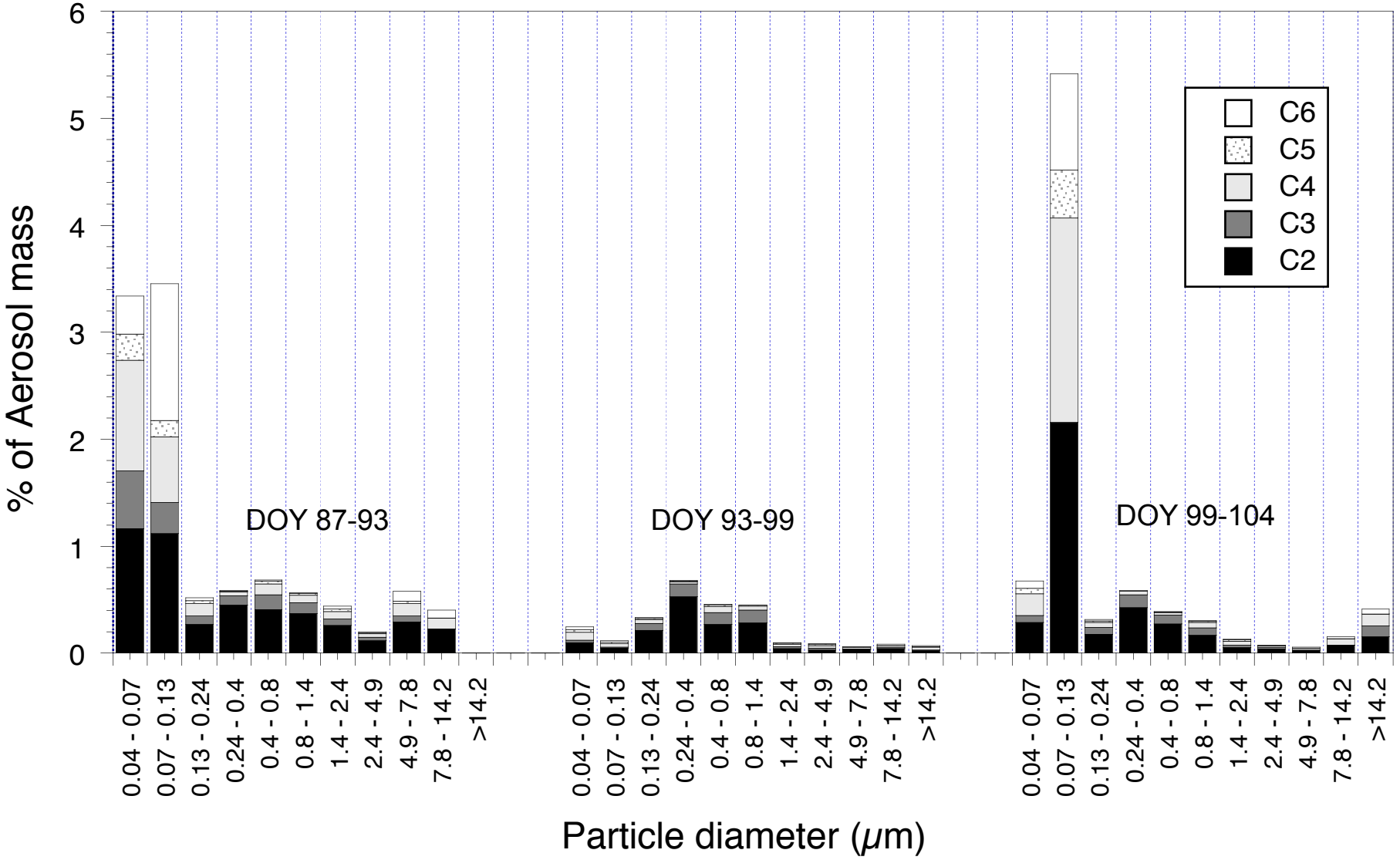

Fig. 6 (Kawamura et al.)

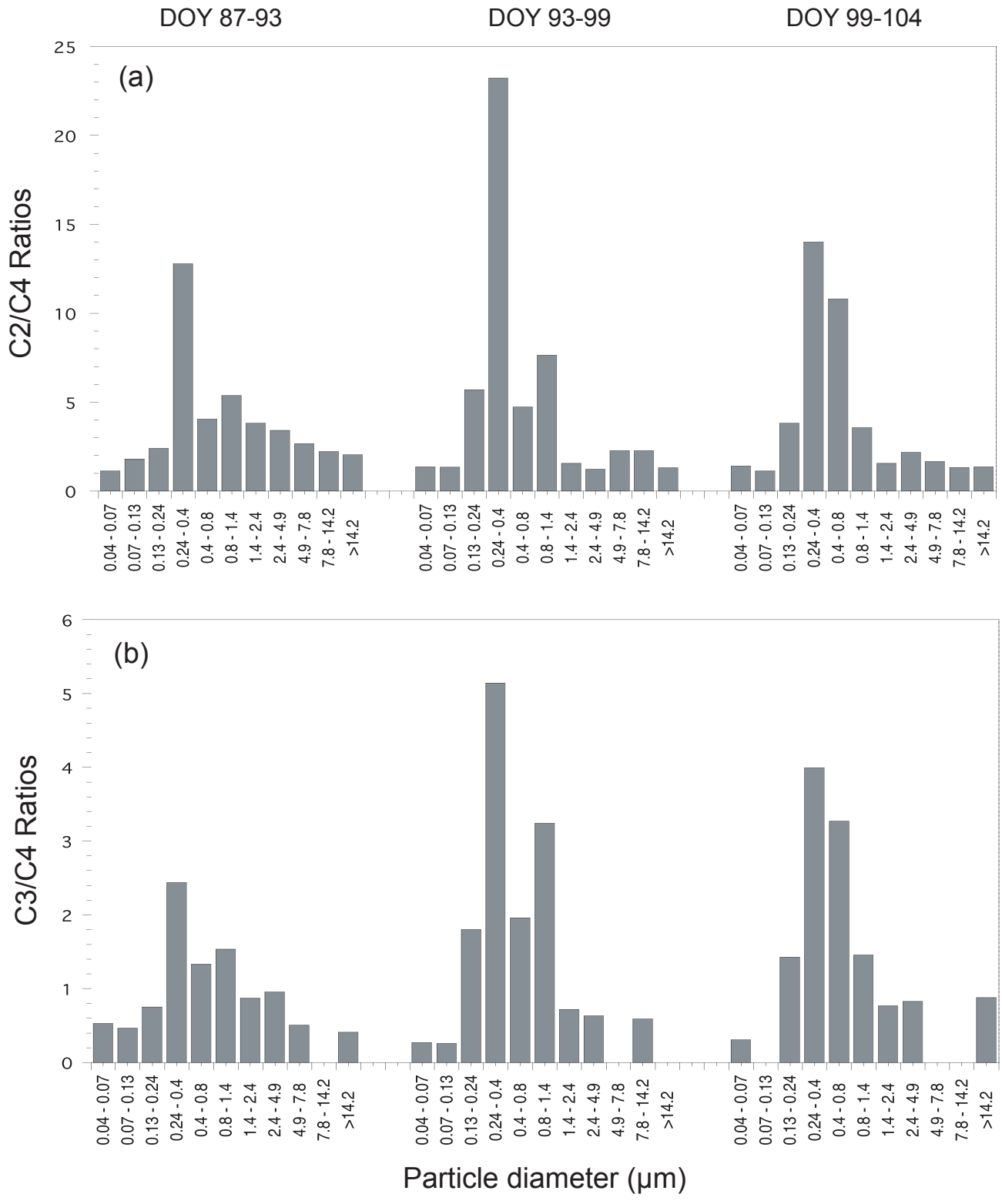

Fig. 7 (Kawamura et al.)